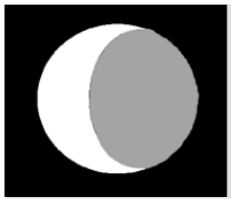

Papers & Presentations

Magmatic Chambers in Cauchy Region: Jansen Mega Dome and Relationship with the Cauchy Volcanic Shield

By Raffaello Lena, coordinator, ALPO Lunar Domes Program, raffaello.lena@alpo-astronomy.org

Abstract

In this study, the wide volcanic region of the Cauchy Shield is examined using Bouguer gravity mass anomaly data, crustal thickness data, Lunar Reconnaissance Orbiter (LRO) Wide Area Camera (WAC) images, the Laser Altimeter Digital Elevation Model (LOLA DEM), and the LRO WAC-based GLD100 Digital Terrain Model (DTM) along with data from the Clementine UVVIS dataset, Chandrayaan-1 Moon Mineralogy Mapper and Kaguya Multiband Imager (MI).

The gravity anomaly data indicates the presence of a frozen magma chamber at low depth in the Jansen complex, like for the Gardner mega dome. Presented here is evidence that the Jansen volcanic complex is another mega dome and possible parasitic volcanic dome of Cauchy Shield located on its periphery. Both features (the Gardner mega dome and the proposed Jansen mega dome) are located on the periphery of the wide Cauchy Shield, which does not display other high gravity anomalies associated with the known lunar domes.

We conclude that on the periphery of the Cauchy Shield two wide frozen magmatic chambers at low depth are present in this volcanic region, characterized by the presence of 56 lunar domes. Finally, the current study describes several volcanic features and suggests the presence of the Jansen mega dome extending for 120 km, with height of 750 m and an average slope angle of 0.8°.

Note to Our Hard-Copy Readers
While the paper version of this Journal is available only in black-and-white, various images in this paper are in full color that can be seen only in the pdf version of this Journal. Contact the ALPO membership secretary for more information.

Introduction

Important clusters of lunar domes are observed in the Hortensius/Milichius/T. Mayer region in Mare Insularum and in Mare Tranquillitatis around the craters Arago and Cauchy (Lena et al., 2013). A first map of terrestrial telescopic images, including the Cauchy domes, has been produced by the author in the lunar domes atlas [http://vitruviuscauchy.blogspot.com]. A classification and description of these domes was performed based on previous works (Lena et al., 2013; Wöhler, Lena et al., 2007; Wöhler, Lena et al., 2006; Lena & Lazzarotti, 2014; Lena & Lazzarotti, 2015). Recently, new global topographic data from the LOLA and LROC instruments on LRO reveal that almost all of the volcanic complexes on the Moon occur on large, regional topographic rises in the lunar maria (Spudis et al., 2013).

The examined domes in Cauchy region are aligned radially with respect to the Imbrium basin. A proposed explanation for these observations is that the domes formed along crustal fractures generated by major impact events, hence running radially with respect to the basin locations (Lena et al., 2013; Wöhler, Lena et al., 2007). Another alternative explanation is that these domes are part of the larger volcanic province of the Cauchy Shield. (Spudis et al., 2013). The alignments of domes, in Cauchy region, are shown in **Figure 1**.

Shield volcanoes typically have both radial and circumferential fissure zones,

Online Readers

Please send comments, questions, observing reports of your own, etc., to the authors by left-clicking your mouse on either of the e-mail addresses under the bylines on this page in blue text.

Also left-click on any hyperlinks in blue text within the text of this paper for additional information.

Observing Scales

Standard ALPO Scale of Intensity:
0.0 = Completely black
10.0 = Very brightest features

Intermediate values are assigned along the scale to account for observed intensity of features

ALPO Scale of Seeing Conditions:
0 = Worst
10 = Perfect

IAU directions are used in all instances.

Lunar Dome Classification System

Effusive Domes

• Class A domes are small and shallow and formed by high-TiO2 lavas of low viscosity, erupting at high effusion rates over very short periods of time, resulting in edifices of low volume.

• Class B domes consist of lavas of intermediate to high viscosity and moderate TiO2 content, erupting at low to intermediate effusion rates. If the effusion process continues over a long period of time, steep flank slopes and high volumes may occur (class B1), while short periods of effusion result in shallower edifices of lower volume (class B2).

• Class C domes are formed out of low-TiO2 (class C1) or high-TiO2 (class C2) lavas building up edifices of large diameter but shallow flank slope. These at shapes are due to low lava viscosities and high effusion rates.

• Class D comprises the very complex, shallow but large and voluminous edifices Arago α and ß, which were most probably formed during several subsequent effusion stages, while classes A-E describe simple, likely monogenetic effusive domes.

• Class E domes represent the smallest volcanic edifices formed by effusive mechanisms (diameter < 6 km). In analogy to class B, the class E domes are subdivided into subclasses E1 and E2, denoting the steep-sided flank slope larger than 2° and the shallow edifices of this class, respectively.

• Class F (empty at this time)

• Class G comprises the highland domes, which have highland-like spectral signatures and high flank slopes of 5°–15°, represented by Gruithuisen and Mairan highland domes.

• Class H is represented by the non-monogenetic Marius domes, subdivided into three different classes. Small domes of less than 5 km diameter belong to subclass H1. The irregular shapes of domes of subclass H2 with more than 5 km diameter and flank slopes below 5° indicate a formation during several effusive episodes. Domes of subclass H3 have diameters compa-rable to those of monogenetic class B1 domes, but their flank slopes are all steeper than 5° and reach values of up to 9°.

• Class I comprises large volcanic shields.

• Class L comprises the Ring Moat Dome (RMDs). These structures are thought to be volcanic in nature, possibly involving the extrusion of magmatic foam.

Putative Intrusive Domes

Lunar domes with very low flank slopes differ considerably from the more typical lunar effusive domes. Some of these domes are exceptionally large, and many of them are associated with faults or linear rilles of presumably tensional origin, while they do not show summit pits. A reliable discriminative criterion is the circularity of the dome outline: these domes are elongated and with low slopes (< 0.9°). The putative intrusive domes have circularity values below 0.8, while the circularity is always higher than 0.9 for the effusive domes having flank slopes below 0.9° and displaying effusive vents.

Class In1 comprises large domes with diameters above 25 km and flank slopes of 0.2°–0.6° and have linear o curvilinear rilles traversing the summit.

Class In2 is made up by smaller and slightly steeper domes with diameters of 10-15 km and flank slopes between 0.4° and 0.9°.

Class In3 comprises low domes with diameters of 13-20 km and flank slopes below 0.3°.

which serve as pathways for magma to get to the surface and erupt lava. Parasitical cone and dome building often occurs near the summit and on the flanks of such features during the latter stages of shield growth (Spudis et al., 2013).

Another volcanic construct, belonging to the Cauchy Shield, is the Gardner mega dome (**figures 1 and 2**) identified by Wood. He proposed the presence of a caldera (the depressed zone at the center of the examined structure), which was the source of lava flows that covered the eastern portion of the mega dome. As described by Wood, *"the break in the southern rim of the caldera appears to be a major drainage area, which carved a channel as lava flooded downhill to the mare"* (Wood at al., 2005). The height of the Gardner mega dome is 1,200 m and its east-west diameter is about 70 km.

The redness of the examined structure is detectable in the Clementine color ratio imagery shown in Figure 3D. The low 415/750 ratio of 0.58 suggests a very low TiO_2 content below 2 wt%, which is confirmed using the Kaguya Multiband Imager (MI) dataset as described later in this paper.

The Gardner mega dome occurs on the northern margin of the Cauchy Shield. Based in part on its alignment with the volcanic area near the crater Jansen, Wood proposed that Gardner is the northern terminus of an elongate quasi-linear volcano-tectonic structure (Wood at al., 2005). More recently, researchers have suggested that Gardner is a possible parasitic shield of Cauchy located on its periphery (Spudis et al., 2013).

This article will describe the results of a study carried out on the Jansen and Gardner region including the analysis of gravity data and the morphometric and spectral characteristics of the examined features.

Bouguer Gravity Anomalies and Crustal Thickness

The analysis of gravity data is a useful approach for characterizing the subsurface crustal and interior structure of a planetary body. Grail dataset obtained by the *Quick Map LRO* global basemap [http://target.lroc.asu.edu/da/qmap.html] has been used for Bouguer gravity mass anomaly (Zuber et al., 2013) and for crustal thickness (Wieczorek et al., 2013).

Eskildsen has produced a gravity anomaly map (**Figure 3**) of the Jansen and Gardner mega dome (Eskildsen, 2022); it shows the gravity anomaly data in the Gardner and Jansen region including the lunar domes in Cauchy. Gravity anomaly mass concentrations are not associated with the majority of the domes in Cauchy region, but are concentrated at the Gardner mega dome and in the vicinity of the crater Jansen. There is also a lesser mass concentration near the craters Sinas and

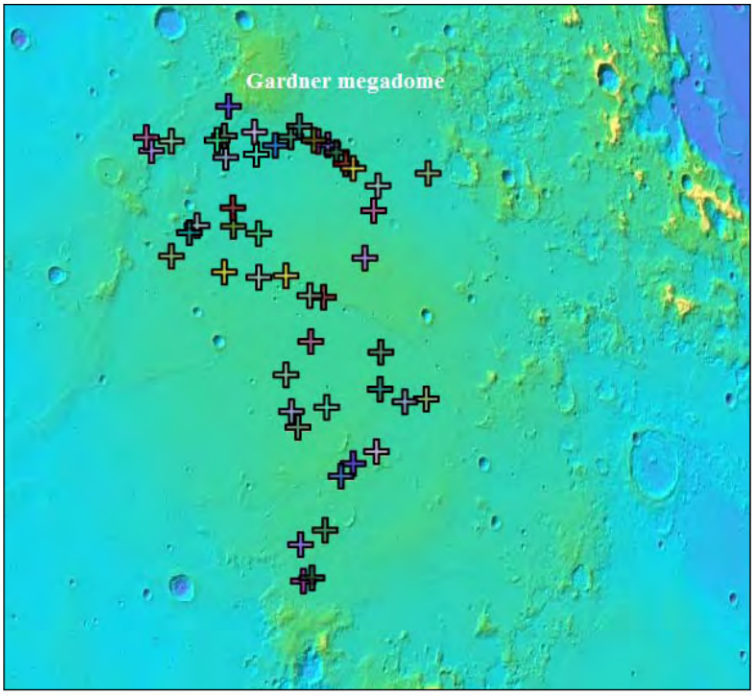

Figure 1. (above left) Cauchy Shield and the aligned domes.

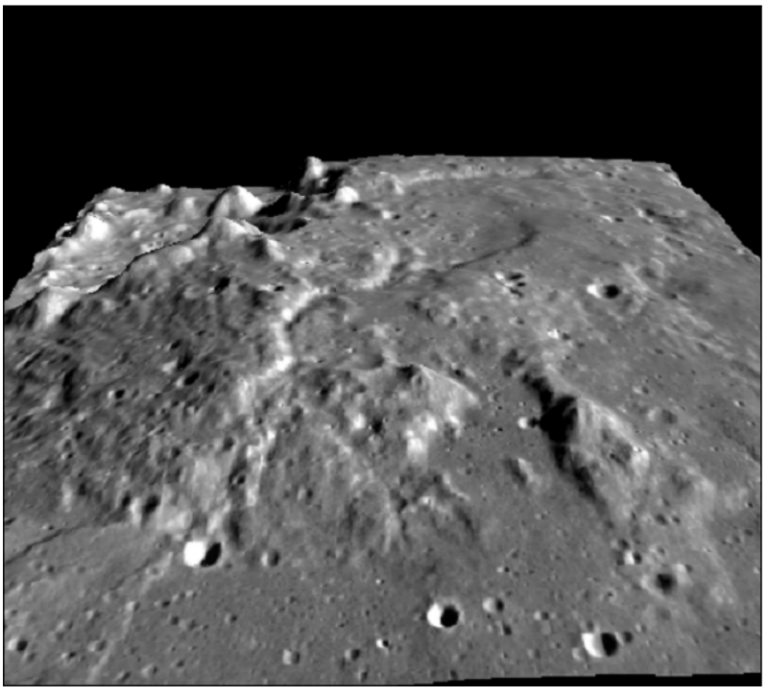

Figure 2. (above right) Gardner mega dome. 3D reconstruction obtained using WAC mosaic draped on top of the global WAC-derived elevation model GLD100.

Sinas E, but no domes are recorded in this area.

The gravity anomaly is shown in red (**figures 3A and 3B**) and is obtained from the GRAIL GRGM900C gravity model after subtracting the gravity resulting from topography assuming a density of 2,550 kg m^{-3}. Consequently these data also indicate variations in thickness of the crust (**Figure 3C**).

The crustal thickness is inferred from the Bouguer gravity map. If the density of the crust is assumed to be uniform, then the gravity anomalies visible in the Bouguer gravity map can be explained by variations in the thickness of the crust (Wieczorek et al., 2013). Highs in gravity indicate places where the mantle is closer to the surface, and hence where the crust is thinner. The gravity anomaly indicates two possible frozen magma chambers at low depth for the Gardner and Jansen region. Thus, is the Jansen another distinct mega dome? A discussion this hypothesis follows below.

Estimated Age

ACT-REACT *Quick Map* tool was used to access to the mare age units. In the corresponding map of the Jansen region, each polygon includes the unit name and age based on the crater size-frequency distribution model (Hiesinger et al. 2011). The model indicates an age of 3.75-3.76 billion years for the Jansen complex. Most of the basalts of the Cauchy region have derived ages of 3.6 billion years and thus younger than the Jansen complex and the Gardner mega dome, for which Spudis suggested an age older than 3.8 billion years [Spudis et al., 2013].

Morphometric Properties

Considering the Jansen region as a unique and complex structure, its elevation is 750 m, the base diameter is determined to be 120 km, while the average slope angle of the complex is 0.8°. Its edifice volume was estimated as about 4,240 km^3 assuming a parabolic shape. A LRO WAC-derived surface elevation plot of the proposed mega dome is shown in **figures 4 and 5**.

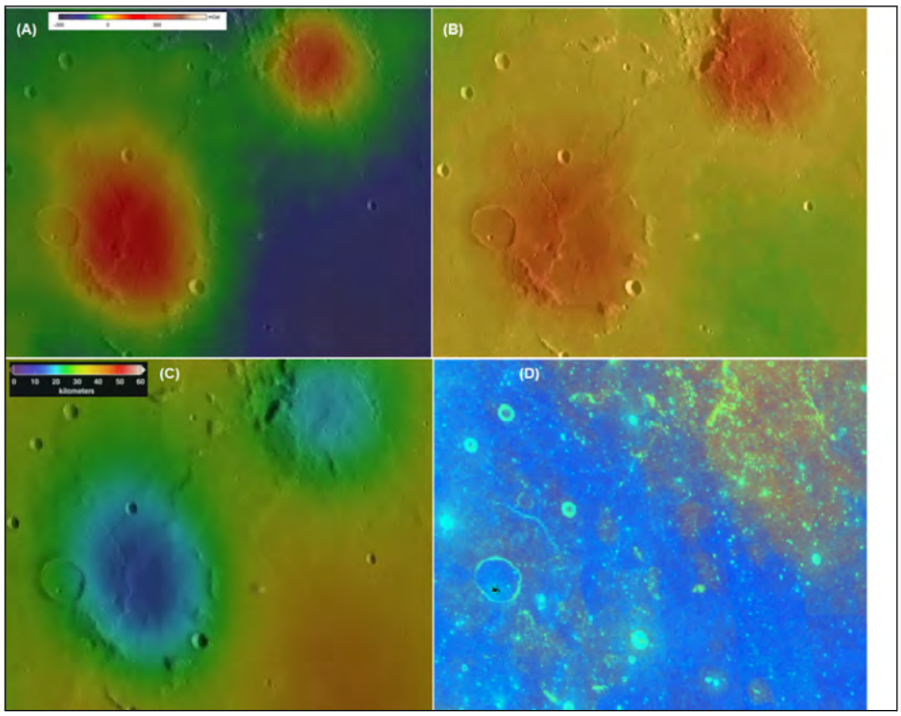

Figure 3. (above left) (A) Bouguer gravity gradients of the examined region. (B) The Grail free air gravity. They show the 'free air' variations as measured by the spacecraft, and thus include contributions from both the surface relief and any sub-surface interfaces. (C) GRAIL crustal thickness map at 16 pixels/degree. It includes shaded relief of surface features. (D) Clementine color ratio image. Channel Ratio: Red = 750 nm/ 415 nm; Green = 750 nm/950 nm; and Blue = 414 nm/750 nm. The lunar highlands, mostly old (~4.5 billion years) gabbroic anorthosite rocks, are depicted in shades of red. The lunar maria (~3.9 to ~1 billion years), mostly iron-rich basaltic materials of variable titanium contents, are portrayed in shades of yellow/orange (iron-rich, loIr titanium) and blue (iron-rich, higher titanium). Superimposed on and intermingled with these basic units are materials from basins and craters of various ages, ranging from the dark reds and blues of ancient basins to the bright blue crater rays of younger craters.

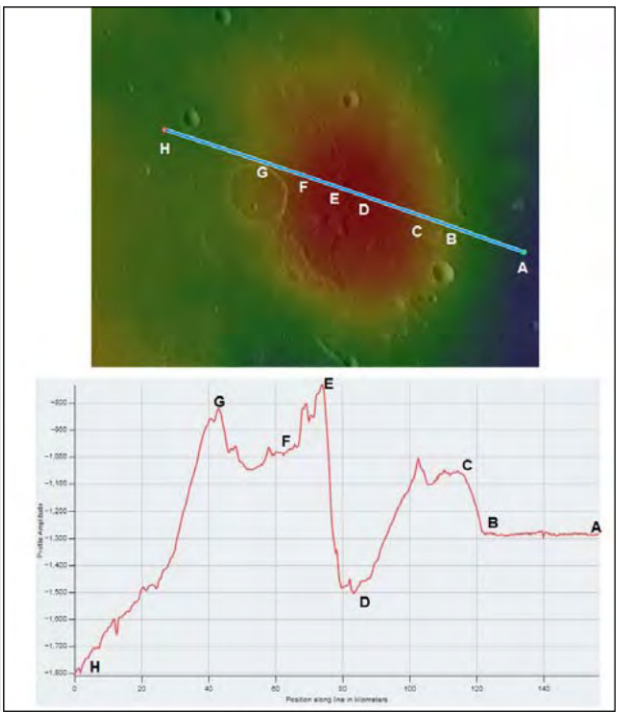

Figure 4. (above right) (Top) gravity gradient of the examined region near Jansen complex where the gravity anomaly is shown in red color indicating places where the denser mantle is closer to the surface. The Bouguer gravity gradient is overlaid on the LOLA DEM. (Bottom) the cross elevation profile of the examined construct, which extends for 120 km.

Volcanic Features of the Jansen Volcanic Complex

A long sinuous rille on its surface, at the centre of the complex, known as *Rima Jansen*, is associated with a *cobra head* indicating lava effusion. Sinuous rilles are formed by thermal and mechanical erosion in association with high-volume, high-effusion rate and long-duration eruptions.

The sinuous rille does start on the summit of this large construct and is traversing the surface, in a NW direction, ending near the surrounding mare unit to the north-west (**figures 5 and 6**). Long wrinkle ridges indicate that compression forces also occurred (**Figure 6**).

Three effusive domes termed C8 and C18-C19 (Lena et al., 2013) are located on its periphery indicating possible different effusive activities. Based on the model age described by Hiesinger at al. (2011), the domes C8 and C18 have an age of 3.75 billion years, while for C19 the model displays an age of 3.69 billion years.

Based on the boundaries of this complex structure (**Figure 4**), this writer suggests the presence of a possible mega dome extending for 120 km and that likely originated, in the initial step, by an intrusion from a subsurface magmatic body. This was followed by successive effusive eruptions, including the formation of three separate lunar domes, interpreted as parasitical domes. Some linear rilles (**figures 4 and 5**) located

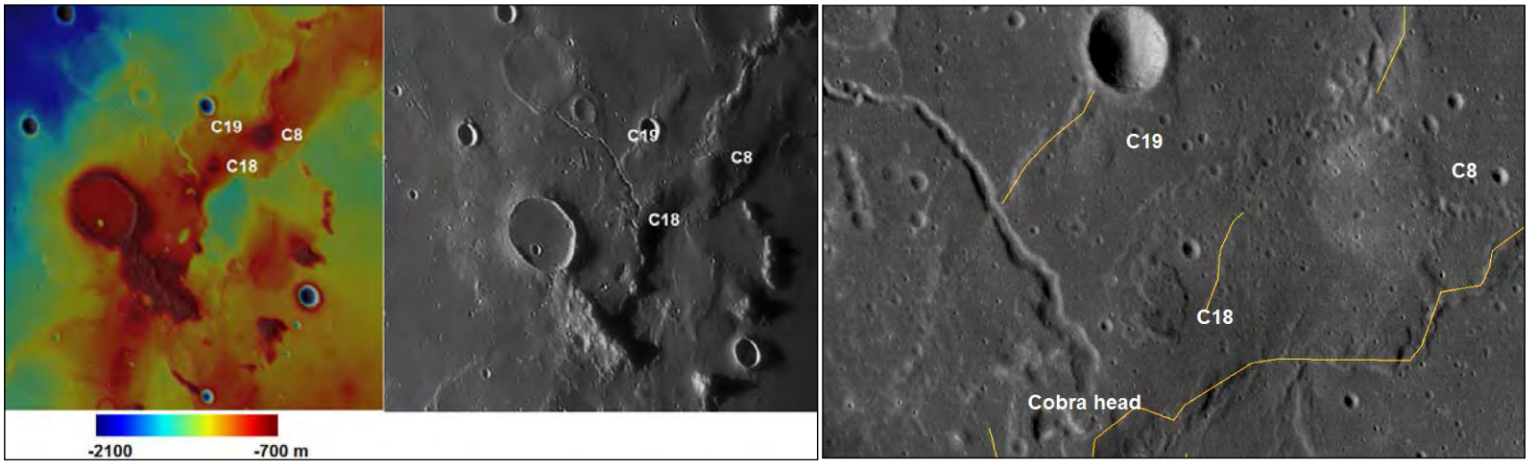

Figure 5. (above left) (Left) elevation of the proposed Jansen mega dome on digital terrain model, including three lunar domes belonging to the volcanic construct and named C8, C18 and C19; (right) telescopic image of the examined region taken by Lazzarotti (September 17, 2011 at 03:48 UT Gladius XLI Cassegrain with aperture of 400 mm f/16 and a Baader Zeiss 2x Barlow lens). The domes C8, C18 and C19 are marked. The telescopic image displays a raised soil of the Jansen complex. In addition, the Jansen complex is more elevated in the west than in the east.

Figure 6. (above right) WAC imagery showing the three domes, named C8, C18 and C19, wrinkle ridges (yellow lines) and a prominent and long sinuous rille originating from a "cobra head."

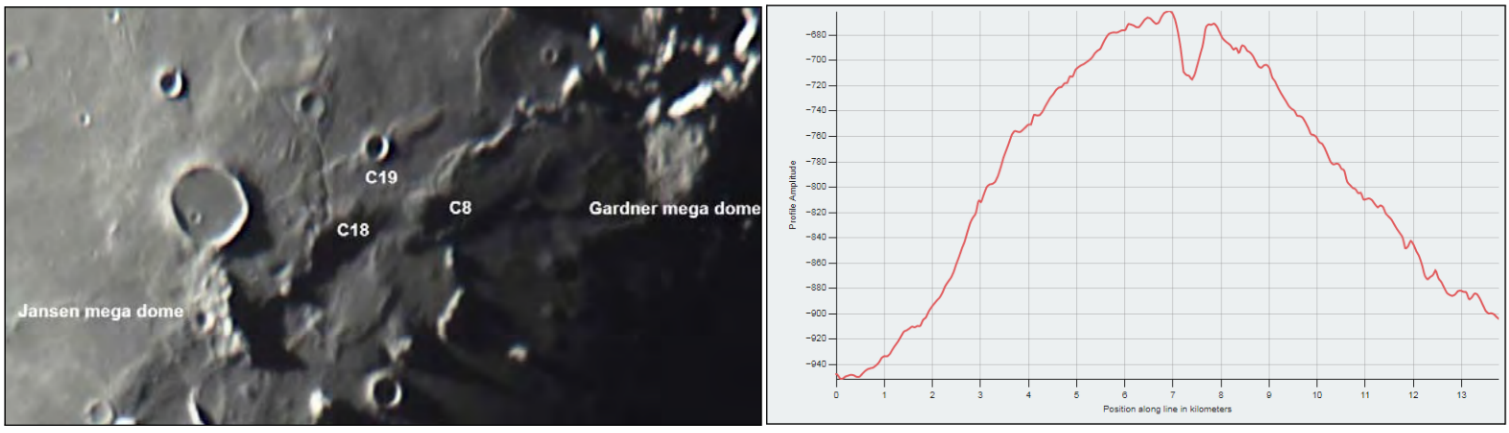

Figure 7. (above left) Jansen mega dome. Image taken by Massimo Dionisi on June 19, 2022 at 01:42 UT. Newtonian reflector 250 mm.

Figure 8. (above right) Dome C8. Cross-sectional profile in E-W direction.

near the crater Jansen E and belonging to the examined volcanic construct are likely expression of tensional stress produced by a magmatic intrusion.

Ground-Based Telescope Observations

The image shown in **Figure 5** displays a overview of the surface of the Jansen complex. The image was taken under oblique solar illumination angle by Lazzarotti on September 17, 2011, at 03:48 UT using a Gladius XLI Cassegrain with an aperture of 400 mm, f/16. The domes C8, C18 and C19 are marked.

Another image of the Jansen complex was taken by Massimo Dionisi on June 19, 2022, at 01:42 UT using a Newtonian reflector with aperture of 250 mm (**Figure 7**).

Further telescopic images (**figures 15 through 17**) are described at the end of this paper.

Compositional Analyses

The FeO content was estimated utilizing the Japan Aerospace Exploration Agency Kaguya spacecraft's Multiband Imager (MI) data; the MI is a high-resolution, multispectral imaging instrument onboard Kaguya. It has five visible (VIS) bands (415 nm, 750 nm, 900 nm, 950 nm, and 1,000 nm) and four near-infrared bands (1,000 nm, 1,050 nm, 1,250 nm, and 1,550 nm).

Estimates of TiO_2 wt% are given from a linear correlation between the TiO_2 contents of returned lunar soil samples and the WAC 321/415nm ratio at the sampling sites: the 321/415nm ratio map was converted to the TiO_2 abundance map as reported by Sato et al. (2017).

Note that the examined region is not fully covered by the Kaguya MI data. However, the derived surface composition indicates an average FeO content ~17–19 wt%, while the TiO_2 content varies from 4.5 wt% to 10.0 wt% indicating different effusive episodes characterized by lava effusion of different composition regarding the titanium content (**Figure 9**). The domes C8 and C19 show lower TiO_2 content (5-7 wt%) than the dome C18 (8.5-9.6 wt%). The *cobra head* displays TiO_2 content of about 8.4 wt%. The abundance of orthopyroxene ranges from 26 wt% to 35 wt% and the abundance of clinopyroxene amounts from 29 wt% to 49 wt%.

Domes of the Jansen Volcanic Complex and Morphomeric Properties

C8 is located at 30.7° E and 14.3° N. It has a base diameter of 13 km and a height of 270 m, yielding an average slope angle of 2.5° (**Figure 8**). Based on spectral and morphometric properties, it belongs to class C_2 of the lunar domes classification (Lena et al., 2013). The TiO_2 content of C8, like the northern dome C19, is 5.4 wt% - 6.6 wt%, indicating a lower abundance than the nearby bluer lavas with a TiO_2 content of 8.4 wt% - 9.6 wt% (**Figure 9**).

C18 has a base diameter of 7.3 km and height of 125 m, yielding an average slope angle of 1.9° (**Figure 10**). It is located at 30.0° E and 14.0° N. Based on the spectral and morphometric properties it belongs to class C_2 of the lunar domes classification (Lena et al., 2013). The TiO_2 content of C18 is 9.5 wt%. On the summit C18 displays an escarpment rising for about 100 m.

Another low dome, C19, is located at 29.9° E and 14.4° N. It has a diameter of 4.0 km, its height is 90 m and the average slope angle is 2.1° (**Figure 11**). The TiO_2 content of C19, like C8, is 5 wt% - 7 wt% (**Figure 9**). It belongs to

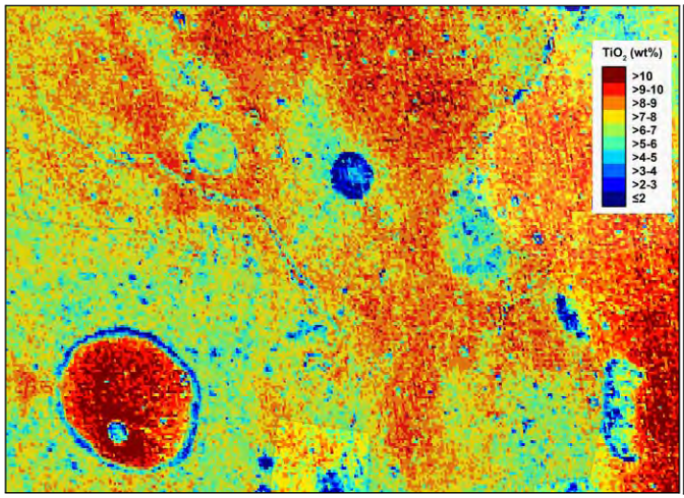

Figure 9. (above left) TiO_2 abundance map in wt% of the examined region.

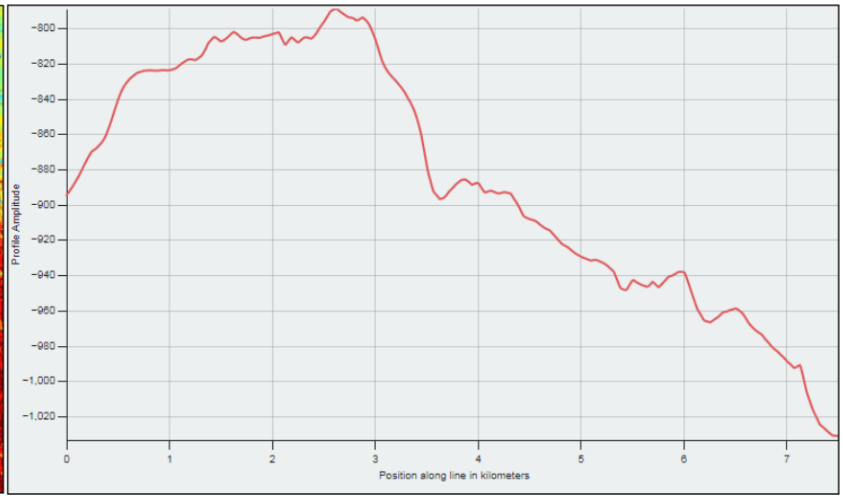

Figure 10. (above right) The dome C18. Cross-sectional profile in E-W direction.

class E_1 of the lunar domes classification. Class E domes represent the smallest volcanic edifices formed by effusive mechanisms (diameter <6 km). The class E domes are subdivided into subclasses E_1 and E_2, denoting the steep-sided flank slopes (larger than 2°) and the shallow edifices of this class, respectively.

The TiO_2 estimation equation reported by Lucey et al. (1998) has also been applied, derived using the Clementine UVNIR dataset, yielding higher values of the titanium abundances. According to this method, the dome C8 displays TiO_2 content between 8.0 wt% and 10.0 wt%. For the dome C18 a value of 10.0 wt% - 11.3 wt% was obtained, while for the dome C19 the TiO_2 content amounts to 9.8 wt% –11.0 wt%.

Results and Discussion

Mineral Types

The Moon Mineralogy Mapper dataset has been used to analyze the mineral

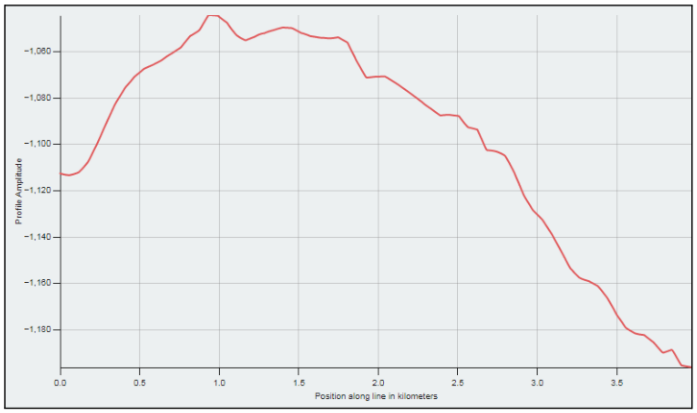

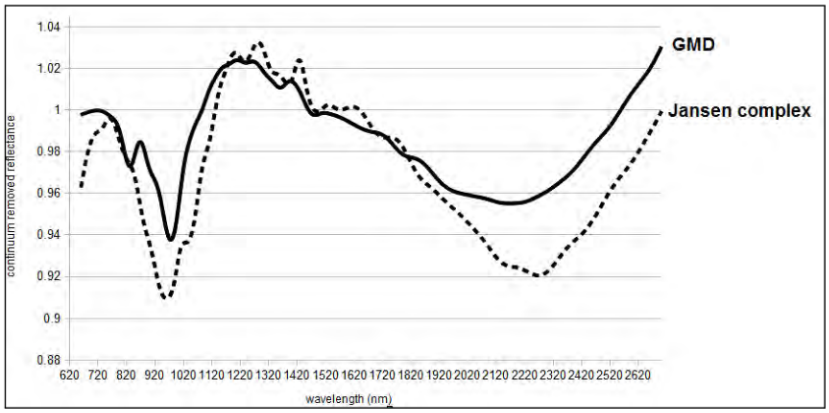

Figure 11. (above left) The dome C19. Cross-sectional profile in E-W direction.

Figure 12. (above right) Spectra for GMD and Jansen complex near the "cobra head."

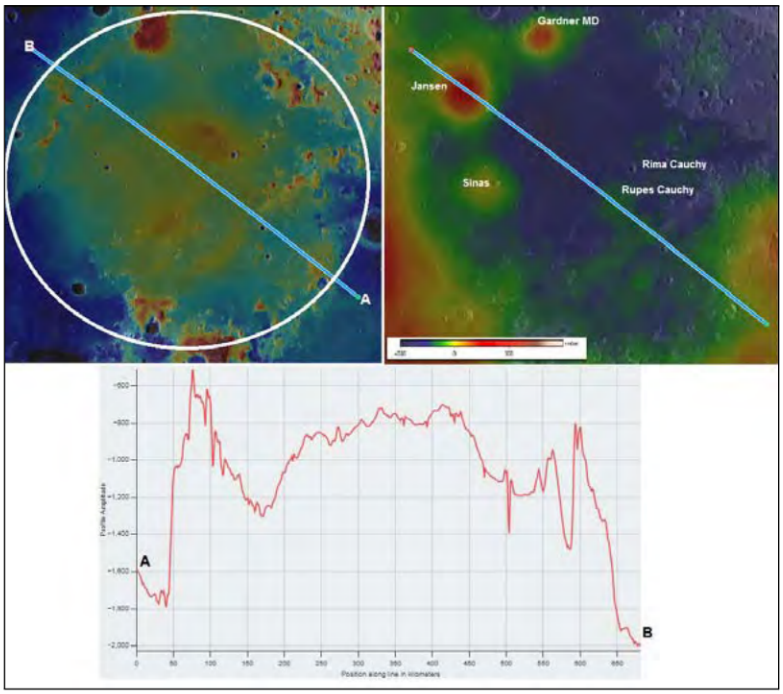

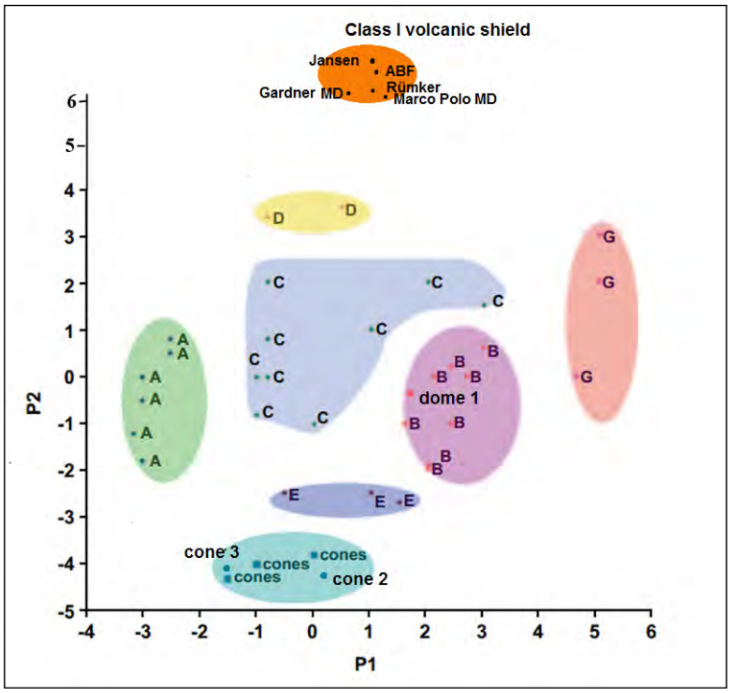

Figure 13. (above left) Top left: Elevation map of the Cauchy Shield. Top right: Map of the Cauchy Shield including the Bouguer anomaly described in the text. Bottom: Topographic profile across line "A-B".

Figure 14. (above right) Classification scheme of effusive lunar mare domes and lunar cones based on a Principal Component Analysis (PCA). Scores P1 and P2 of the features vectors describing the domes on the first two principal components of the data distributions. The dome classes A-E and G (highland domes including Gruithuisen domes) and the lunar cones are indicated. Note that the examined volcanic shields (Gardner MD, Mons Rümker, Marco Polo MD, ABF MD and Jansen volcanic complex) have their specific class (Class I).

composition of the Gardner mega dome (GMD) and the Jansen volcanic complex.

Data from the orbital period OP1B for Jansen and OP2C3 for GMD were calibrated and photometrically corrected and converted to apparent reflectance values. Data have been obtained through the M^3 calibration pipeline to produce reflectance with photometric and geometric corrections. For deriving the spectral parameters, the photometrically corrected Level 2 data of the PDS imaging node have been used. Pyroxenes are characterized by distinct absorption bands around 1,000nm and 2,000nm, with low-calcium pyroxenes (OPX) displaying bands shifted to slightly shorter wavelengths (890nm -940nm and 1,900nm -2,000nm), and high-calcium pyroxenes (CPX) exhibiting bands at slightly longer wavelengths with increasing Ca and Fe (970nm - 1,010nm and 2,150nm - 2,300nm) (Besse et al., 2014). Olivine has a complex absorption centered near 1,000 nm, with no absorption at 2,000nm (Besse et al., 2014). Therefore, olivine-rich lunar deposits are characterized by a broad 1,000nm absorption band (1,030nm - 1,090nm) which is enhanced relative to the 2,000nm band. The 1,000nm band center of lunar glass is generally shifted to longer wavelengths when compared to pyroxene, and the 2,000nm band center to shorter wavelengths. Thus, two 1,000nm and 2,000 nm band center positions of lunar glasses will typically appear closer together than those of pyroxenes (Besse et al., 2014).

The spectra (**Figure 12**) display a typical high-Ca pyroxene signature with a minimum wavelength at 970nm - 980 nm and another absorption band at 2,130nm (for GMD) and 2,300nm (for Jansen); this difference is due to different TiO_2 contents of the sampled area. According to the derived FeO and TiO_2 content for the GMD (~14.0 wt% and ~1.0 wt% in average, respectively), the main rock type is low-Ti basalt with high calcium pyroxene.

For the Jansen mega dome the derived FeO and TiO_2 (from ~5.0 wt% to 9.0 wt% in average) indicate that the main rock type is medium to high-Ti basalts with high calcium pyroxene.

Possible Mega Dome and Volcanic Formation

In the Jansen complex, lunar eruptions probably spanned a range of volumes and mass eruption rates, allowing both shield-building and flood-type eruptions, in different effusive phases.

The intense volcanic activity also formed three single and parasitical domes described above (C8, C18-19). They likely originated from magma ascent by dikes, which erupted lavas. These three domes formed during the later stages of the period of volcanic activity characterized by a decreasing rate of lava extrusion and comparably low eruption temperature, resulting in the formation of small effusive domes. Note that these domes are located on the eastern part of the Jansen volcanic complex.

Based on WAC imagery, a scarp runs up through the surface of the complex (**figures 4 and 5**), suggesting a low-

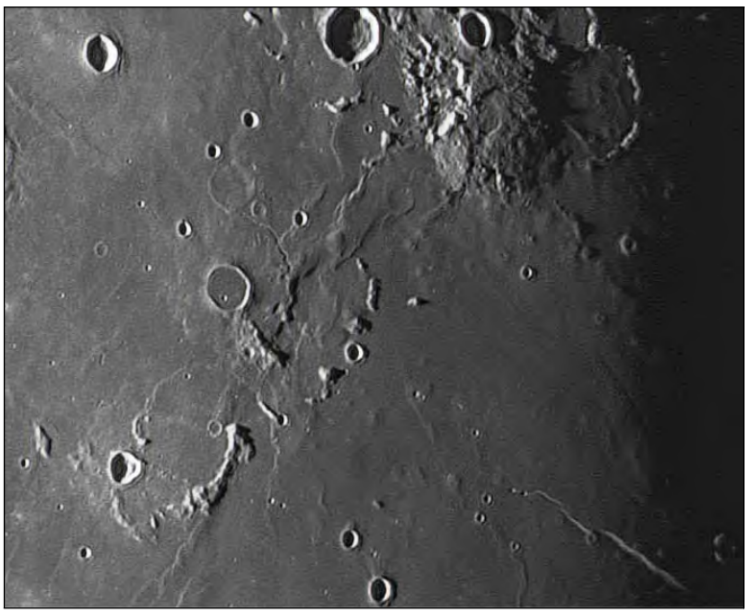

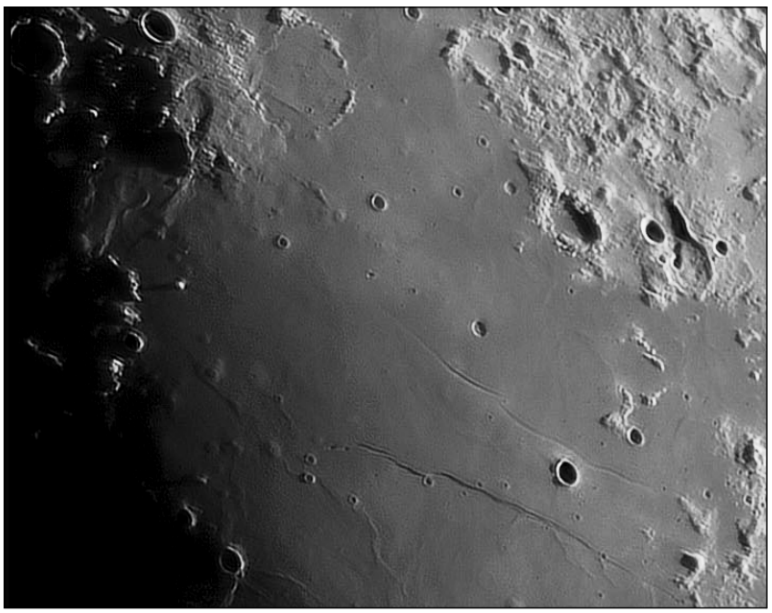

Figure 15. (above left) Gardner, Jansen, Vitruvius and Cauchy region. Image taken by Guy Heinen on August 19, 2019 at 23:57 UT with a Mewlon 250 mm.

Figure 16. (above right) Gardner and Cauchy region. Image taken by Howard Eskildsen on May 6, 2022 at 00:31 UT with a Schimdt Cassegrain 230 mm.

angle thrust fault, with the terrain on the western side overriding that on the eastern side. This might be also consistent with an up-arching of the central part of the surface as a result of an intrusion forming a laccolith within the crust. Moreover, the lava channel originating on the summit from a cobra head has clearly supplied lava to the surrounding maria with eruption of low viscosity in a next and different effusive phase.

The Cauchy Volcanic Shield and Its Relationship with the Proposed Jansen Mega Dome

The Cauchy Shield reported by Spudis et al. (2013) extends for 670 km with a height of 1,700 m (**Figure 13**). Based on the data and analysis in this study, the Jansen mega dome is part of this wide shield.

The volcanic shields Gardner MD, Mons Rümker, Marco Polo MD and the ABF (Apennine Bench Formation) Mega Dome form a separate spectral and morphometric group in the lunar domes classification scheme, based on a Principal Component Analysis (PCA): the volcanic shields (Class I) display a different cluster if compared with the classical effusive domes, the non-monogenetic domes of class D, the highland domes (class G) and the lunar cones (**Figure 14**). Mons Rümker, which is situated in the north-eastern part of Oceanus Procellarum, with a diameter of about 65 km, is the largest contiguous volcanic edifice on the Moon: the height of the plateau is about 900 m in its western and north-western section, 1100 m in its southern section, and 650 m in its eastern and north-eastern part (yielding an average slope of 1.7°) (Wöhler, Lena et al., 2013).

Another typical example of these features is the Marco Polo mega dome (Marco Polo MD), which can be considered as another possible lunar volcanic shield (Lena and FitzGerald, 2017). Based on the boundaries of the ABF, Lena and FitzGerald argue the presence of another possible mega dome extending for 120 km and with an average slope angle of 0.5° (Lena and FitzGerald, 2019). Note that the Jansen volcanic complex, proposed in the current study as another mega dome, belongs to the same cluster of previous described volcanic shield (**Figure 14**).

This writer also proposes that the Jansen volcanic complex is another mega dome and possibly a parasitic shield of the Cauchy Shield located on its periphery, like the Gardner mega dome.

Summary and Conclusion

In this study, I have performed an analysis of the morphologic, morphometric and spectral properties of the Jansen complex, which is recognized as another mega dome, and discussed a chronology of the events, occurred in this complex region, including a phase of uplift occurred likely under the influence of a laccolith like intrusion in the shallow crust. Effusive processes occurred in several effusive eruptions and also originating three domes located in the north east region of the proposed Jansen mega dome.

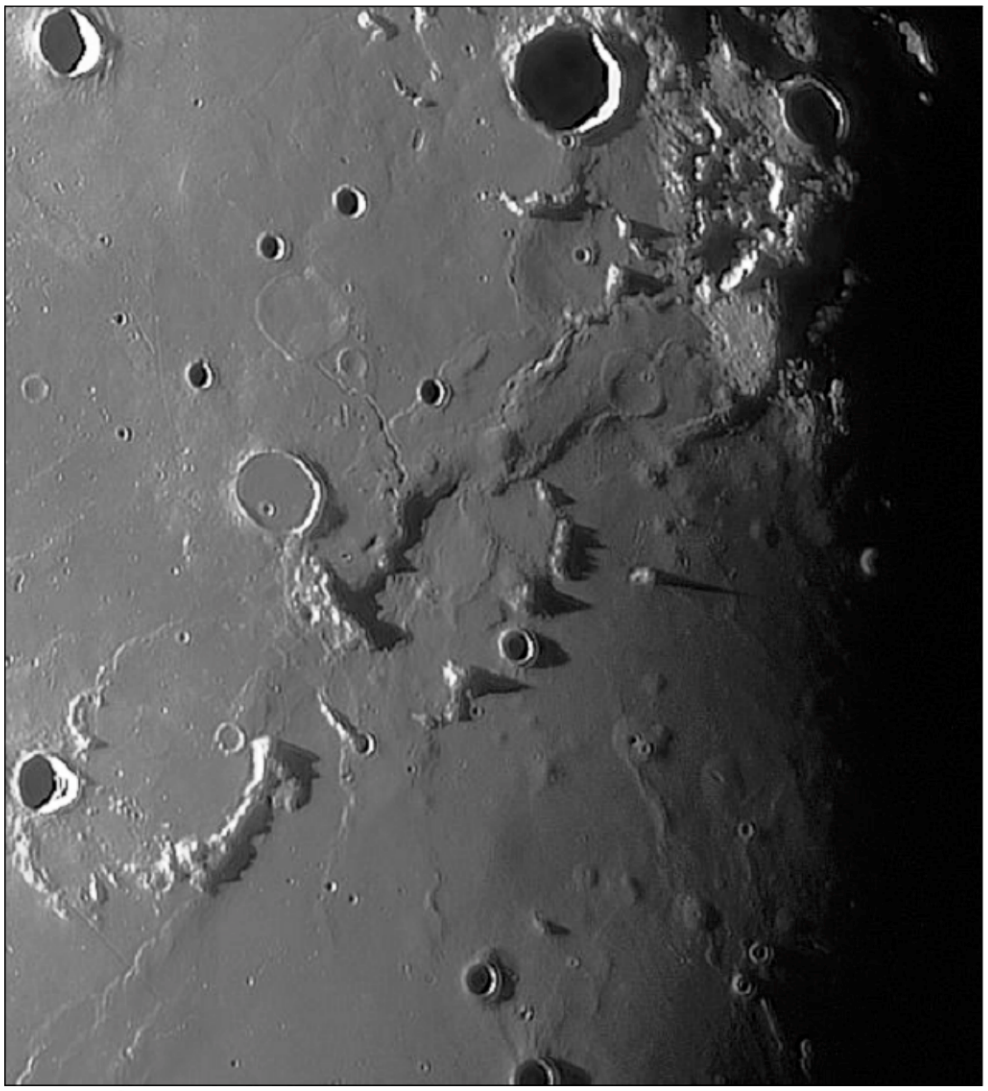

Figure 17. Gardner-Jansen region. Image taken by Howard Eskildsen on September 15, 2022 at 09:38 UT with a Schimdt Cassegrain 230 mm.

The gravity anomaly indicates the presence of another frozen magma chamber at low depth also in the Jansen mega dome (**Figure 13**), like for the Gardner mega dome.

Both of these features are located on the periphery of the wide Cauchy Shield, which does not display other high gravity anomalies associated with the known lunar domes. Thus, only on the periphery of the Cauchy Shield are two wide frozen magmatic chambers at low depth detected in this volcanic region, characterized by the presence of 56 lunar domes, whose distribution and location are shown in our published Cauchy map [http://vitruviuscauchy.blogspot.com].

References

Besse, S., J. M. Sunshine, and L. R. Gaddis (2014), Volcanic glass signatures in spectroscopic survey of newly proposed lunar pyroclastic deposits, *Journal of Geophysical Research: Planets*, 119, doi:10.1002/2013JE004537.

Eskildsen, H. (2022). Jansen and Cauchy Gravity Anomaly Map based on LRO Data, (Personal Communication).

Hiesinger, H., Head III, J. W., Wolf, U., Jaumann, R., Neukum, G. (2011) "Ages and stratigraphy of lunar mare basalts: A synthesis." *Geological Society of America Special Papers* 477, 1-51. doi:10.1130/2011.2477(01). Online at *https://pubs.geoscienceworld.org/gsa/books/book/638/chapter/3806251/Ages-and-stratigraphy-of-lunar-mare-basalts-A*

Lena, R., Wöhler, C., Phillips, J., Chiocchetta, M.T. (2013). *Lunar Domes: Properties and Formation Processes*, Springer Praxis Books. https://www.springer.com/gp/book/9788847026360

Lena, R., Lazzarotti, P., 2014. "Domes in northern Mare Tranquillitatis: Morphometric analysis and mode of formation." *Selenology Today*, 35, 12-24.

Lena, R., Lazzarotti, P., 2015. "Domes in northern Mars Tranquillitatis, near the craters Vitruvius G & M," *Journal of the British Astronomical Association* V. 125, No. 2, 97-104.

Lena, R. and Fitz-Gerald, B. (2017). "The Marco Polo complex: Another possible Lunar Volcanic Shield." *Proceedings of the Lunar and Planetary Science Conference*, Vol. XLVIII abstract 1005.pdf. Online at *https://www.hou.usra.edu/meetings/lpsc2017/pdf/1005.pdf*

Lena, R. and FitzGerald, B. (2019) "A lunar survey of the Apennine Bench Formation & identification of volcanic features." *Journal of the British Astronomical Association*, V.129, No. 6, 329-340.

Lucey, P.G., Bleltt, D.T., Hawke, B.R., (1998) "Mapping the FeO and TiO_2 content of the lunar surface with multispectral imagery." *Journal of Geophysical Research* 103 (E2), 3679–3699.

Sato, H., Robinson, M.S., Lawrence, S.J., Denevi, B.W., Hapke, H., Jolliff, B.L., Hiesinger, H. (2017) "Lunar Mare TiO_2 Abundances Estimated from UV/Vis Reflectance." *Icarus*, doi:10.1016/j.icarus.2017.06.013.

Spudis, P. D., P. J. McGovern and W. S. Kiefer (2013). "Large shield volcanoes on the Moon." *Journal of Geophysical Research: Planets*, 118, 1063–1081, doi:10.1002/jgre.20059.

Wieczorek, M. A., G. A. Neumann, F. Nimmo, W. S. Kiefer, G. J. Taylor, H. J. Melosh, R. J. Phillips, S. C. Solomon, J. C. Andrews-Hanna, S. W. Asmar, A. S. Konopliv, F. G. Lemoine, D. E. Smith, M. M. Watkins, J. G. Williams, M. T. Zuber, "The crust of the Moon as seen by GRAIL." *Science*, 339, 671-675, doi:10.1126/science.1231530, 2013.

Wöhler, C., Lena, R., & Phillips, J., (2007). "Formation of lunar mare domes along crustal fractures: Rheologic conditions, dimensions of feeder dikes, and the role of magma evolution." *Icarus*, 189 (2), 279–307.

Wöhler, C., Lena, R., Lazzarotti, P., Phillips, J., Wirths, M., & Pujic, Z. (2006). "A combined spectrophotometric and morphometric study of the lunar mare dome fields near Cauchy, Arago, Hortensius, and Milichius." *Icarus*, 183, 237–264.

Wöhler, C., Lena, R., Pau, K.C. (2007). "The Lunar Dome Complex Mons Rümker: Morphometry, Rheology, and Mode of Emplacement." *Lunar and Planetary Science Conference Proceedings* XXXVIII. #1091.

Wood, C. A., Higgins, W., Pau, K.C., Mengoli, G. (2005). "The Lamont-Gardner megadome alignment: A lunar volcano-tectonic structure?" *Lunar and Planetary Science Conference Proceedings* XXXVI, 1116.

Zuber, M. T., Smith, D. E., Watkins, M. M., Asmar, S. W., Konopliv, A. S., Lemoine, F. G., Melosh, H. J., Neumann, G. A., Phillips, R. J., Solomon, S. C., Wieczorek, M. A., Williams, J. G., Goossens, S. J., Kruizinga, G., Mazarico, E., Park, R. S. and Yuan, D. (2013). "Gravity field of the Moon from the gravity recovery and interior laboratory (GRAIL) mission." *Science* 339 668–671, *https://doi.org/10.1126/science.1231507*.